

## Supplementary Information

### Novel Drug Delivery Nanosystems Based on Out-inside Bifunctionalized Mesoporous Silica Yolk-shell Magnetic Nanostars Used as Nanocarriers for Curcumin

Peilin Huang<sup>‡a</sup>, Baozhen Zeng<sup>‡b</sup>, Zhuoxian Mai<sup>a</sup>, Juntao Deng<sup>a</sup>, Yueping Fang<sup>a</sup>, Wenhua Huang<sup>‡b</sup>, Hongwu Zhang<sup>‡b</sup>, Jinying Yuan<sup>c</sup>, Yen Wei<sup>c</sup>, Wuyi Zhou<sup>\*a</sup>

<sup>a</sup> Institute of Biomaterial, Department of Applied Chemistry, College of Materials and Energy, South China Agricultural University, Guangzhou, 510642, China;

<sup>b</sup> Department of Anatomy, Guangdong Provincial Key laboratory of Construction and Detection in Tissue Engineering, Southern Medical University, Guangzhou 510515, China

<sup>c</sup> Key Lab of Organic Optoelectronics & Molecular Engineering of Ministry of Education, Department of Chemistry, Tsinghua University, Beijing, 100084, China

Corresponding authors, Email: Wuyi Zhou, [zhouwuyi@scau.edu.cn](mailto:zhouwuyi@scau.edu.cn); Hongwu Zhang, [zhanghwu@mail2.sysu.edu.cn](mailto:zhanghwu@mail2.sysu.edu.cn); Wenhua

[Huang.huangwenhua2009@139.com](mailto:Huang.huangwenhua2009@139.com)

<sup>‡</sup> Both authors contributed equally to this work

#### 1. Synthesis of Water-based Ferrofluid

The water-based ferrofluid was prepared as follows. The Fe<sub>3</sub>O<sub>4</sub> nanoparticles was firstly prepared through a co-precipitation method as our previous work. Briefly, 4.00 g of FeCl<sub>2</sub> and 5.40 g of FeCl<sub>3</sub> were dissolved in 26 mL hydrochloric acid solution with HCl/water (1/25), and ultrasound for 15 min in a reactor, and then 180 mL of NaOH solution (1.5 M) was added dropwise until the black precipitation generated with vigorous stirring at 800 rpm in the atmosphere of nitrogen. The reaction was kept for another 1 h and the obtained Fe<sub>3</sub>O<sub>4</sub> nanoparticles were collected with the association of the magnetite and then washed by water and ethanol triply, and finally re-dispersed in aqueous solution. The pH value of the solution was adjusted to 6.0 by addition of 0.1 M of critic acid and the water-based ferrofluid was prepared with concentration of 0.025 g/mL. The TEM image of Fe<sub>3</sub>O<sub>4</sub> nanoparticles in water-based ferrofluid were shown in Fig .S1.

#### 2. Drug Release in *Vitro* Pharmacokinetics of Drug Delivery Nanosystems

Release mechanisms in *vitro* of drug deliver nanosystems were determined by the selected three kinds of release kinetic statistic models described as follows.

Zero-order model was applied to drug delivery nanosystems with a constant release rate which had no associated with drug concentration in release media. The equation for zero order release can be expressed as:

$$M_t / M_\infty = kt \quad (1)$$

Since release rate only depending on the concentration of drug in media in some circumstances, first order model could be applied to explain the release mechanism of the drug delivery nanosystems following Fick's law. The equation for first order release can be described as:

$$\ln(1-M_t / M_\infty) = -kt \quad (2)$$

Release pharmacokinetics of drug delivery naosystems, fabricated by insoluble porous materials as matrix system, was commonly described by Higuchi models, which were based on a square

root of a time and process of Fickian diffusion.

$$M_t / M_\infty = kt^{0.5} \quad (3)$$

In above equations,  $M_t$  and  $M_\infty$  represented the amount of drug release at time  $t$  and the final maximum, respectively. Meanwhile,  $k$  is the corresponding release rate constant.

### 3. Cell Culture

Human embryonic kidney (HEK) 293T cells, human liver cancer (SK-HEP1) cells and HepG2 cells were cultured and maintained in Dulbecco's modified Eagle's medium (DMEM) (GIBCO, Invitrogen, USA) with 10% fetal bovine serum (FBS), 1% penicillin-streptomycin at 37 °C in humidity atmosphere containing 5% CO<sub>2</sub>. Medium was replaced every 2 days. When grown to 80 ~ 90% confluence, cells were passaged by repeated trypsinization (0.25% trypsin/0.02% EDTA for 2 ~ 3 min) and replanting. Cell numbers were determined with an electronic cell counter device (CASY1, Schärfe Systems, Reutlingen, Germany).

### 4. Hemolysis Assay

The blood samples from healthy adult rats were used to evaluate the blood compatibility of NS, M<sub>2</sub>NS, F<sub>0.6</sub>NS and F<sub>0.6</sub>M<sub>2</sub>NS. Rat red blood cells (RBCs) were collected by removing the serum from the blood after centrifugation and suction. RBCs were purified by washing with PBS five times, and then diluted to 1/10 of their initial volume with PBS solutions. A 0.5 mL suspension of diluted RBCs suspension was then mixed with 1.0 mL 0.9% NaCl as a negative control; 1.0 mL 10% Triton-100 as a positive control; or 1.0 mL of NS, M<sub>2</sub>NS, F<sub>0.6</sub>NS and F<sub>0.6</sub>M<sub>2</sub>NS suspension (0.9% NaCl) at concentrations ranging from 31.2 to 2000 µg/mL. The mixtures were shaken slightly and then kept still for 2 h at room temperature. The samples were centrifuged, photographed, and the absorbance of the supernatants at 570 nm was measured in a microplate reader (Bio Tek Instruments, Inc.). All experimental protocols and animal handling procedures were approved by the Institutional Animal Care and Use Committee of Southern Medical University (Guangzhou, China) and in accordance with the National Institutes of Health Guide for the Care and Use of Laboratory Animals.

### 5. Cell Apoptosis Study

Microscopic fluorescence images of the 293T and SK-HEP1 cells were obtained using an upright fluorescence microscope (Olympus, BX51, Tokyo, Japan). The 293T and SK-HEP1 cells were cultured and maintained in NS, M<sub>2</sub>NS, F<sub>0.6</sub>NS and F<sub>0.6</sub>M<sub>2</sub>NS for 48 h at concentrations ranging from 31.25 to 2000 µg/mL and normal DMEM for 36 h, and then it was stained with Hoechst33342 for nucleus and analyzed using ImagePro Plus 6.0 software (Media Cybernetics, Bethesda, MD, USA). And cell apoptosis of free curcumin, Cur@F<sub>0.6</sub>NS and Cur@F<sub>0.6</sub>M<sub>2</sub>NS were studied with SK-HEP1 cells according to the dosage of curcumin with concentrations from 7.8 to 31.25 µg/mL, using the same conditions above.

### 6. Cell Viability Study

The cytotoxicity of NS, M<sub>2</sub>NS, F<sub>0.6</sub>NS or F<sub>0.6</sub>M<sub>2</sub>NS against different cell lines, including 293T and SK-HEP1 cells was evaluated *in vitro* using the Cell Counting Kit-8 (CCK-8) (Dojindo, Kumamoto, Japan), according to the manufacturer's manual. In brief, 293T and SK-HEP1 cells were seeded in a 96-well plate at a density of  $2.5 \times 10^3$  cells per well. DMEM (100 µL) containing

10% FBS was added to each well, and incubated for 24 h (37 °C, 5% CO<sub>2</sub>). The medium was aspirated off, and then each well was washed three times with 1× PBS. Fresh medium (100 µL) containing NS, M<sub>2</sub>NS, F<sub>0.6</sub>NS and F<sub>0.6</sub>M<sub>2</sub>NS in PBS at different concentrations (2000 µg/mL, 1000 µg/mL, 500 µg/mL, 250 µg/mL, 125 µg/mL, 62.5 µg/mL, 31.2 µg/mL), was added in triplicate. The liquid was aspirated off after a 48 h incubation and replaced with 100 µL of fresh medium and 10 µL of CCK-8 reagent. The cells were further incubated for 2h, and then the absorbance at 570 nm was measured in a microplate reader (Bio Tek Instruments, Inc.). Negative controls were 293T and SK-HEP1 cells incubated without any treatment of nanospheres. The cytotoxicity was expressed as the percentage of cell viability compared to untreated controls. Meanwhile, the cytotoxicity of different drugs' formulations, i.e., free curcumin, Cur@F<sub>0.6</sub>NS and Cur@F<sub>0.6</sub>M<sub>2</sub>NS were evaluated through the same method above, incubation with SK-HEP1 cells and HepG2 cells according to the dosage of curcumin (125 µg/mL, 62.5 µg/mL, 31.2 µg/mL, 15.6 µg/mL, 7.8 µg/mL) for 48 h.

### 7. Confocal laser scanning microscopy (CLSM)

SK-HEP1 cells were plated at a density of 1×10<sup>4</sup> cells/well in 6-well plates containing sterile cover slips and grown at 37 °C for overnight. The cells were then incubated with free curcumin, Cur@F<sub>0.6</sub>NS and Cur@F<sub>0.6</sub>M<sub>2</sub>NS with concentration equal to the dosage of curcumin 31.2 µg/mL for 1 h or 4h. The cover slips were then washed three times with PBS and blocked in glycerinum. Cover glass was visualized under a laser scanning confocal microscope (Olympus, FV1000). In order to evaluate the intercellular release properties of curcumin under alternative magnetic fields, the SK-HEP1 cells were incubated with Cur@F<sub>0.6</sub>M<sub>2</sub>NS with the same dosage above by applying the alternative magnetic field (1500 mT at the alternative frequency of 120 rpm) at different time intervals such as 15, 30 and 45 min.

### 8. DTA and TG analysis

The thermal gravity of template removed NS and M<sub>2</sub>NS were found to be almost constant up to 800 °C in Fig. S7(a), and weight loss of S-NS and S-M<sub>2</sub>NS was attributed to the decomposition of surface functionalized organic groups, which were measured as 21.4 % for S-NS and 21.7 % for S-M<sub>2</sub>NS corresponded to the remove of surface modified thiol groups HS-(CH<sub>2</sub>)<sub>3</sub>-, which were very closed to theoretical value 23.3 %. Observed in Fig. S7(a), the weight losses of F<sub>0.6</sub>NS and F<sub>0.6</sub>M<sub>2</sub>NS were attributed to decomposition of both thiol groups and bone chains of *Si-β*-CD molecules, the total weight loss values were measured as 48.6 % for F<sub>0.6</sub>NS and 47.0 % for F<sub>0.6</sub>M<sub>2</sub>NS, and the weight losses of organic groups of functionalized *Si-β*-CD molecules were closed to 30 %, and the theoretical value was measured as 31.4 %. The thermal properties of *β*-CD, F<sub>0.6</sub>NS and F<sub>0.6</sub>M<sub>2</sub>NS were similarly showed in Fig. S7(a). In Fig. S7(b), the theoretical weight loss of Cur@F<sub>0.6</sub>NS and Cur@F<sub>0.6</sub>M<sub>2</sub>NS were more than 40 % since the drug loading capacity were measured as 10.1±2.4 % for Cur@F<sub>0.6</sub>NS and 9.8±1.8 % for Cur@F<sub>0.6</sub>M<sub>2</sub>NS, the results were precisely reflected in Fig. S7(b). The DTA curves could also describe the decomposition of surface functionalized molecules concretely. Seen in Fig. S7(c), the template removed NS and M<sub>2</sub>NS did not produce any thermal effect when the temperature increased. The exothermic peaks of S-NS, S-M<sub>2</sub>NS at 349.7 °C, 352.9 °C corresponded to the decomposition of thiol groups in Fig. S7(c). Meanwhile, the endothermic effect at 327.0 °C and exothermic effect at 414.1 °C of *β*-CD was observed according to the decomposition of the organic bone chains. The endothermic peak at

317.4 °C and exothermic peak at 365.6 °C of  $F_{0.6}M_2NS$  were attributed to the decomposition of thiol groups and *Si-β*-CD groups. The endothermic peak at 334.7 °C and the exothermic peak at 413.3 °C of  $F_{0.6}NS$  were considered to be the decomposition of surface *Si-β*-CD molecules. However, the exothermic peak of decomposition of thiol groups was not obviously which might be caused by the endothermic effect of decomposition of *Si-β*-CD at near 350 °C. The endothermic effect of curcumin molecules were observed clearly in Fig. S7(d) for pure curcumin at 188.0 °C corresponded to the sharp melting peak. The peaks of  $Cur@F_{0.6}NS$  at 180.5 °C and  $Cur@F_{0.6}M_2NS$  at 178.3 °C. The shift of the peaks of  $Cur@F_{0.6}NS$  and  $Cur@F_{0.6}M_2NS$  to lower temperature might be due to the formation of curcumin in both drug delivery nanosystem through the drug loading process as the nano crystal formation, which might lower the melting point of curcumin. The weaker crystallized degree of  $Cur@F_{0.6}M_2NS$  were shown in Fig. S7(d) compared with  $Cur@F_{0.6}NS$ , corresponding to the weaker endothermic peak in the DTA curves.

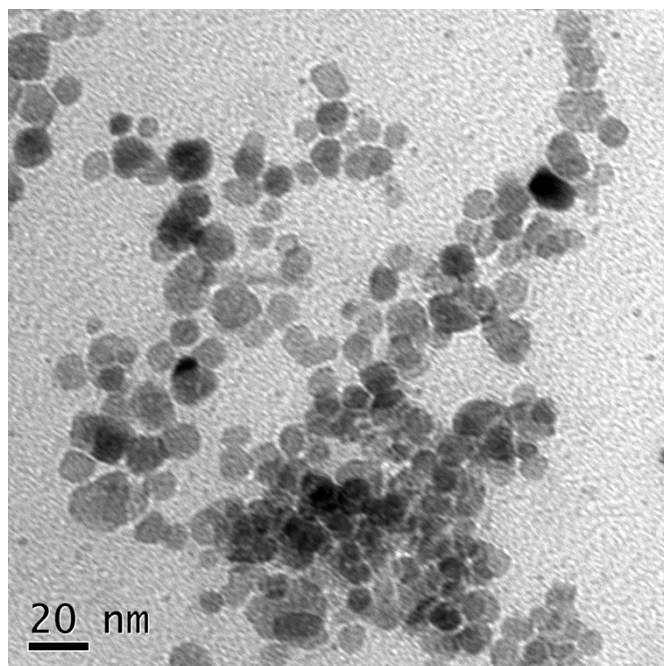


**Fig .S1** TEM image of water-based ferrofluid

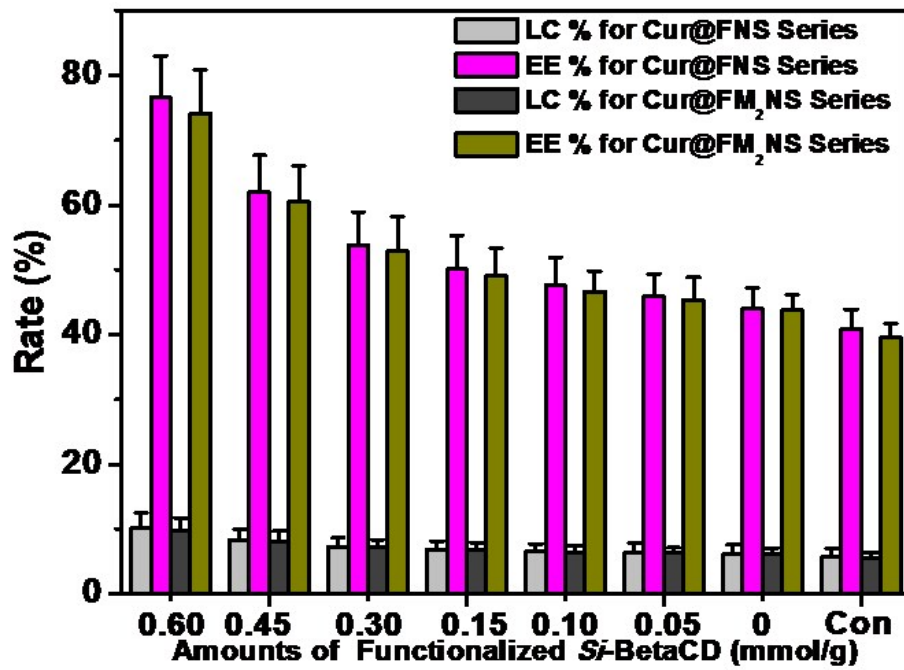


Fig .S2 Drug loading capacity and entrapment efficiency of different samples

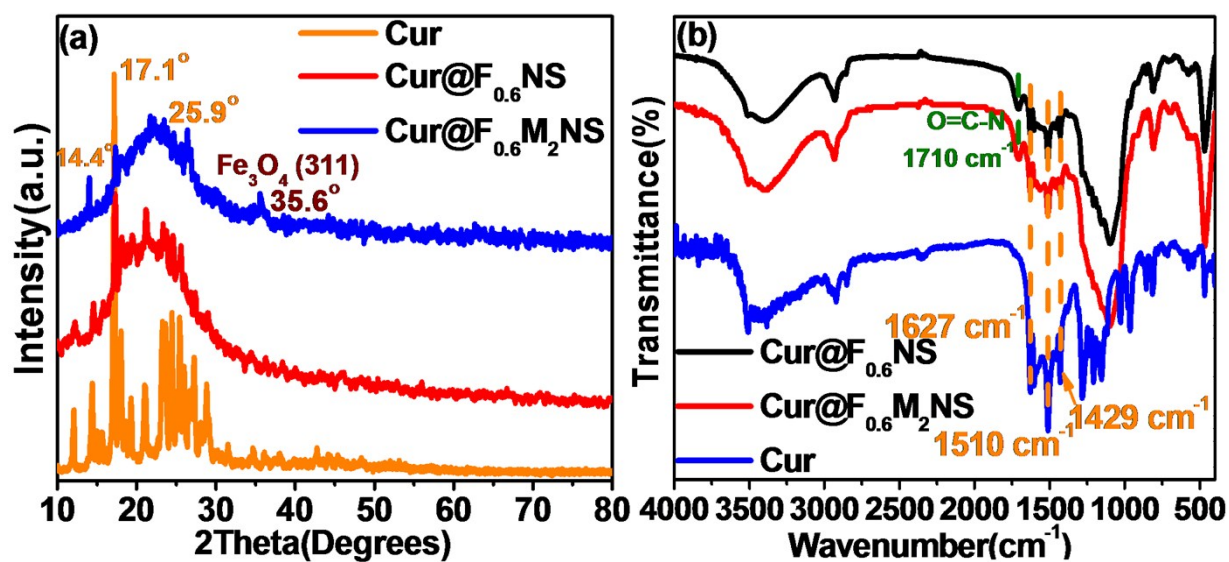


Fig. S3 Physical properties of different drug delivery formulations, (a) XRD patterns; (b) FT-IR patterns

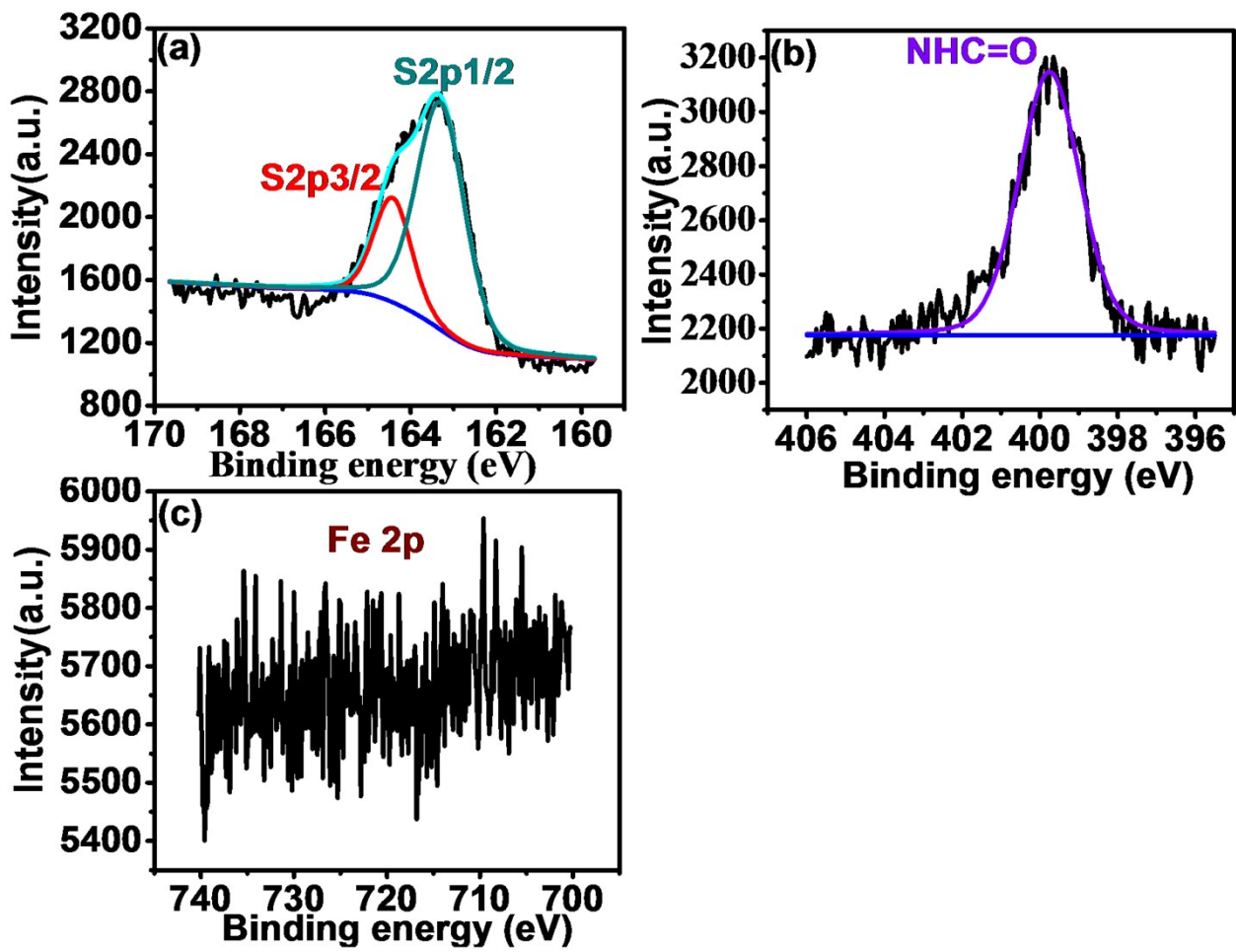


Fig .S4 The XPS S2p spectrum of  $F_{0.6}M_2NS$  (a), N1s spectrum of  $F_{0.6}M_2NS$  (b) and Fe2p spectrum of  $F_{0.6}M_2NS$  (c)

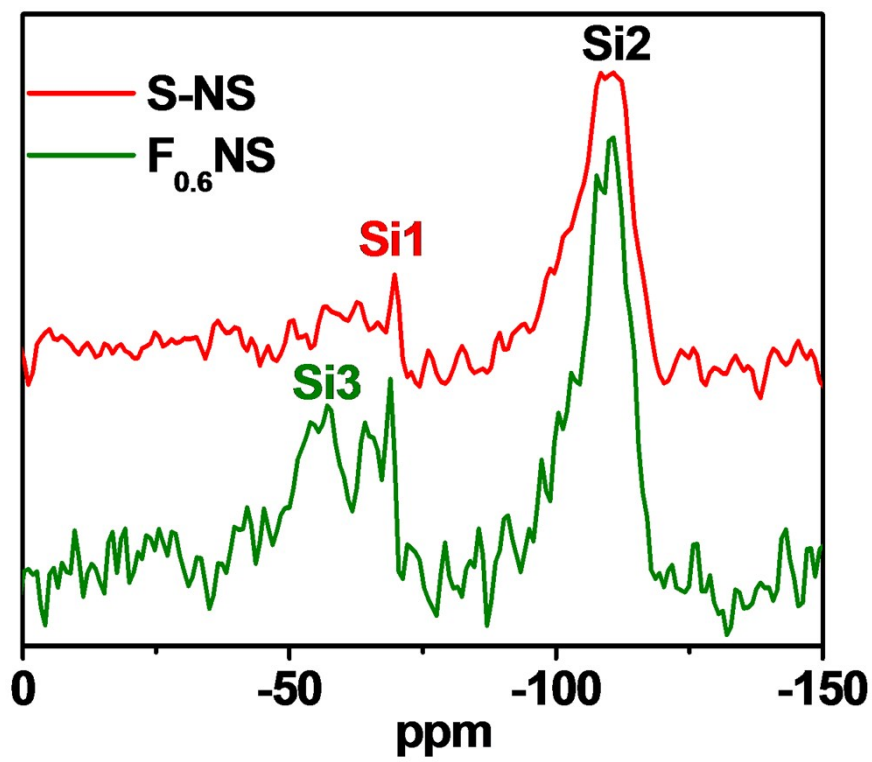


Fig. S5  $^{29}\text{Si}$  NMR spectra for S-NS and  $\text{F}_{0.6}\text{NS}$

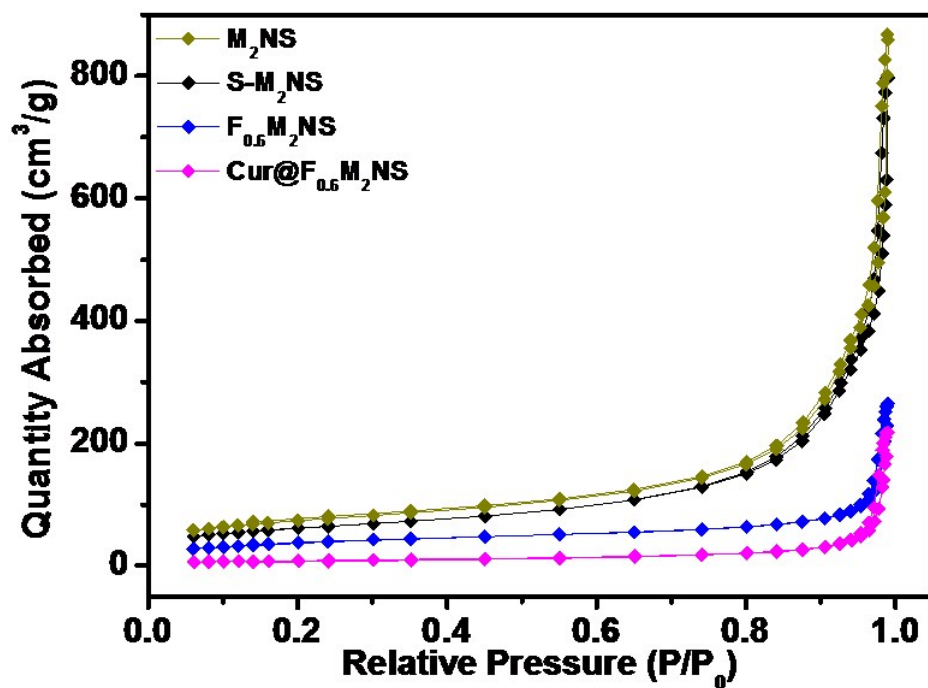


Fig .S6 Nitrogen adsorption-desorption isotherms of different samples

Table .S1 BET surface area and aperture parameters of magnetic nanostar various samples

Sample	M <sub>2</sub> NS	S-M <sub>2</sub> NS	F <sub>0.6</sub> M <sub>2</sub> NS	Cur@F <sub>0.6</sub> M <sub>2</sub> NS
BET surface area (m <sup>2</sup> g <sup>-1</sup> )	256.62	215.27	134.81	30.46
Pore diameter (nm)	24.29	23.54	21.15	12.34
Pore volume (cm <sup>3</sup> g <sup>-1</sup> )	0.88	0.83	0.28	0.22

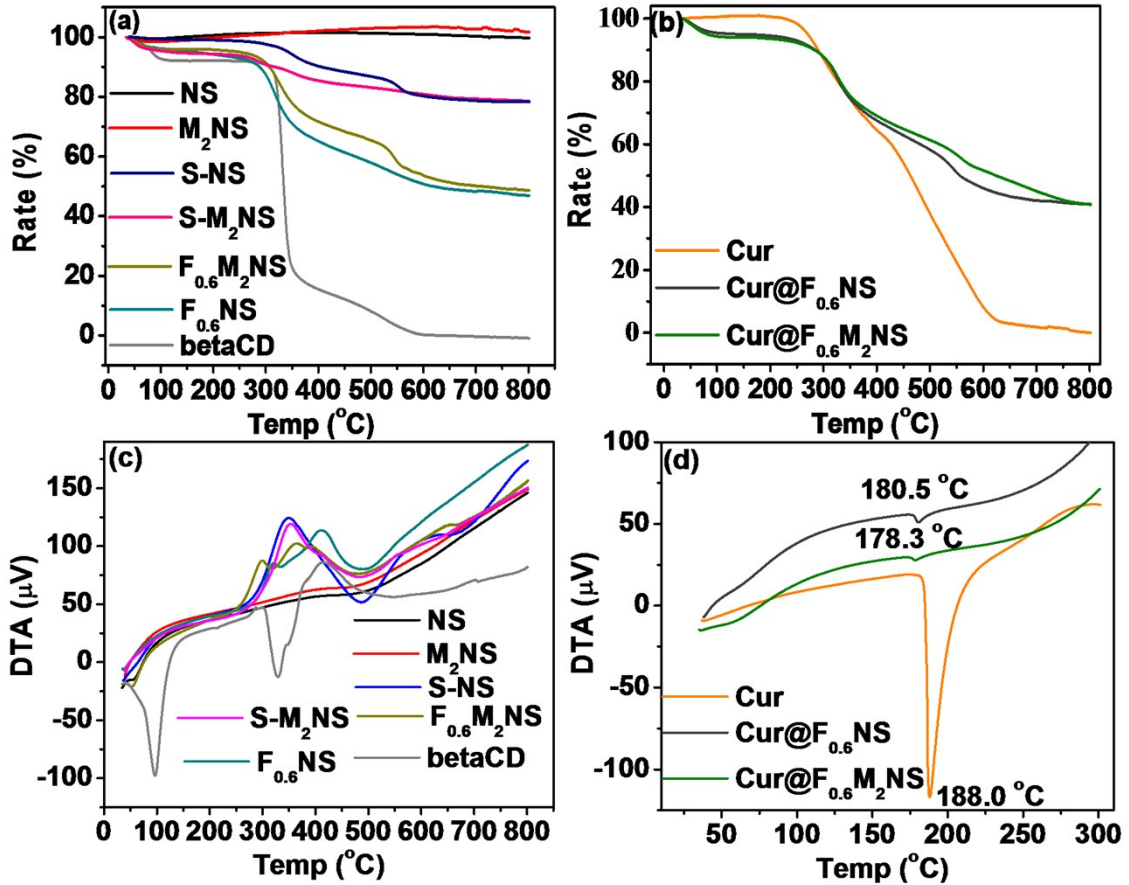
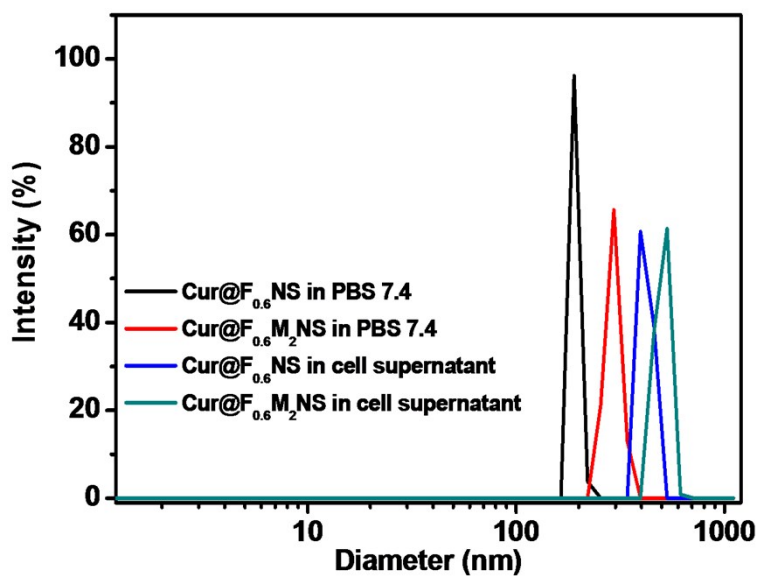


Fig. S7 Thermal properties analysis of different samples, TG curves of different samples (a) (b), DTA curves of different samples (c) (d).



**Fig .S8** The size distribution graph at scattering angle of 90° in of different drug delivery nanosystems in different medium with concentration of 6% wt.

**Table .S2** Parameters in DLS experiment

Media	Drug delivery nanosystems	Z-average diameter (nm)	PDI	ζ-potential (mV)
PBS 7.4	Cur@F <sub>0.6</sub> NS	249.09	0.300	-35.4
	Cur@F <sub>0.6</sub> M <sub>2</sub> NS	299.07	0.201	-35.3
Cell supernatant	Cur@F <sub>0.6</sub> NS	420.16	0.203	-21.0
	Cur@F <sub>0.6</sub> M <sub>2</sub> NS	471.97	0.180	-17.0

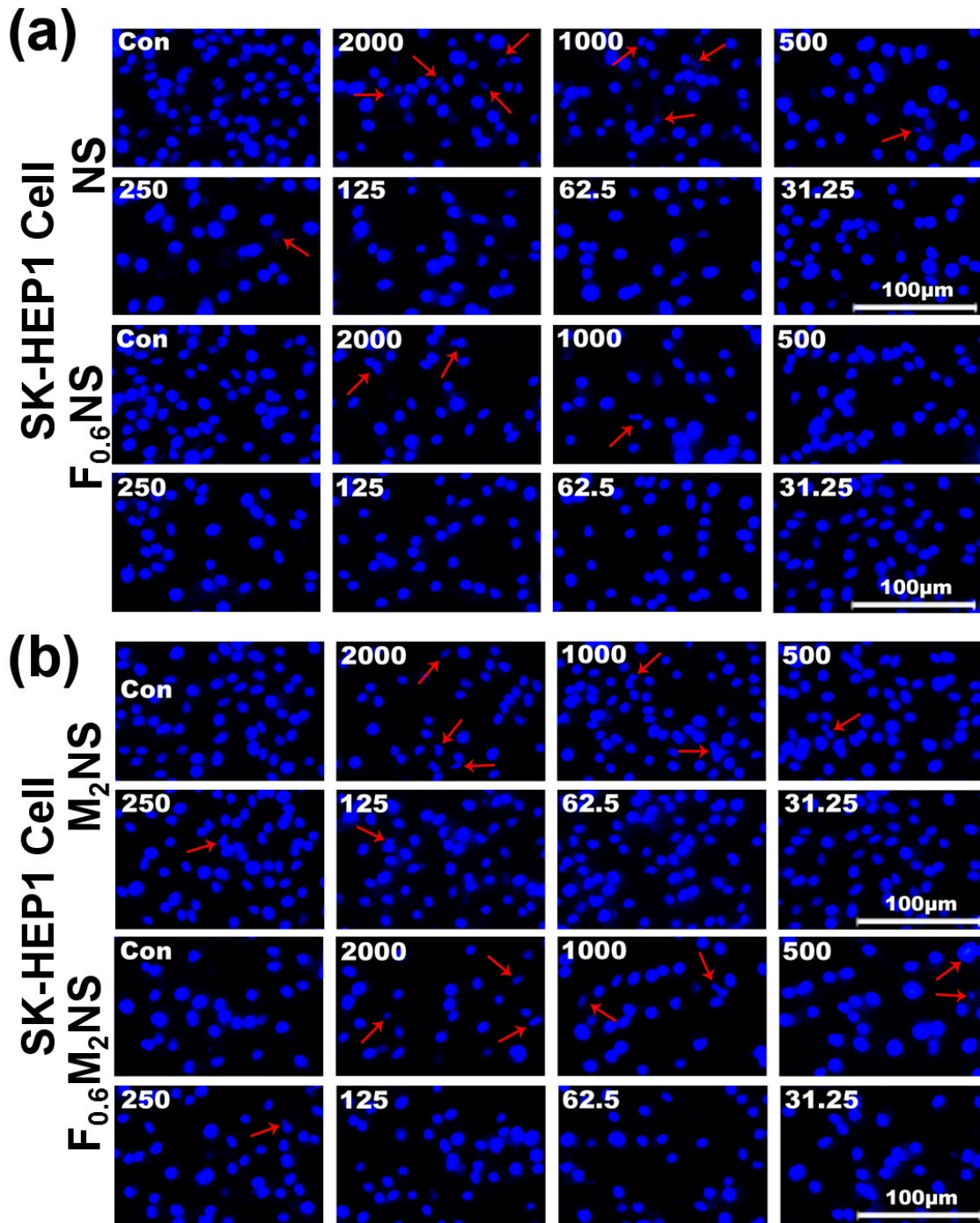


**Fig .S9** Immunofluorescence microscopy analysis of apoptosis in SK-HEP1 cells induced by NS and F<sub>0.6</sub>NS (a), and M<sub>2</sub>NS and F<sub>0.6</sub>M<sub>2</sub>NS (b) at different concentrations (ranging from 31.25 to 2000 μg/mL) for 48 h. Red arrows indicated apoptosis cells. These drug delivery materials did not have any significant effect on the nucleuses (blue) stained with Hoechst 33342. Scale bar: 100 μm.

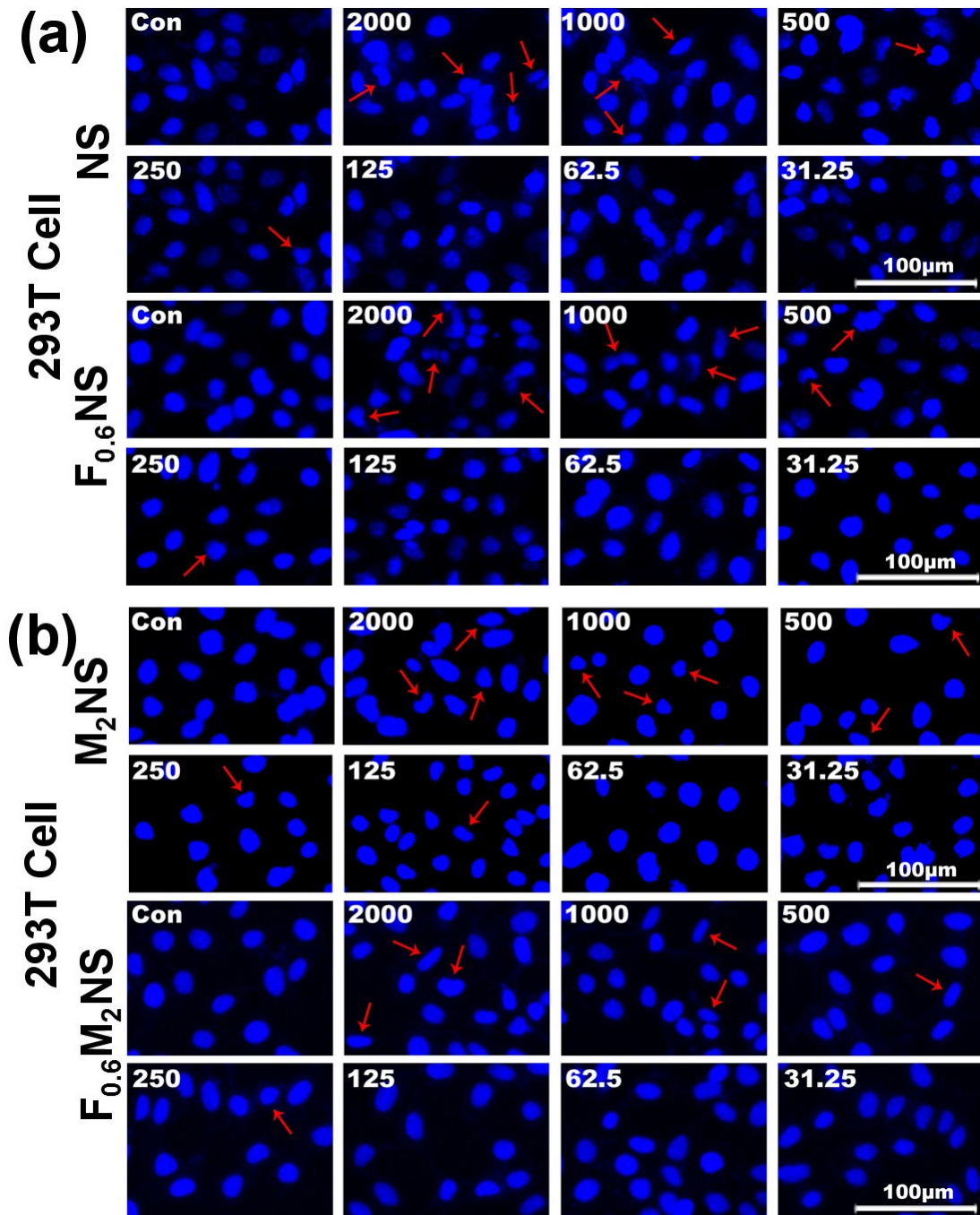


**Fig .S10** Immunofluorescence microscopy analysis of apoptosis in 293T cells induced by NS and F<sub>0.6</sub>NS(a), and M<sub>2</sub>NS and F<sub>0.6</sub>M<sub>2</sub>NS (b) at different concentrations (ranging from 31.25 to 2000 μg/mL) for 48 h. Red arrows indicated apoptosis cells. These drug delivery materials did not have any significant effect on the nucleuses (blue) stained with Hoechst 33342. Scale bar: 100 μm.

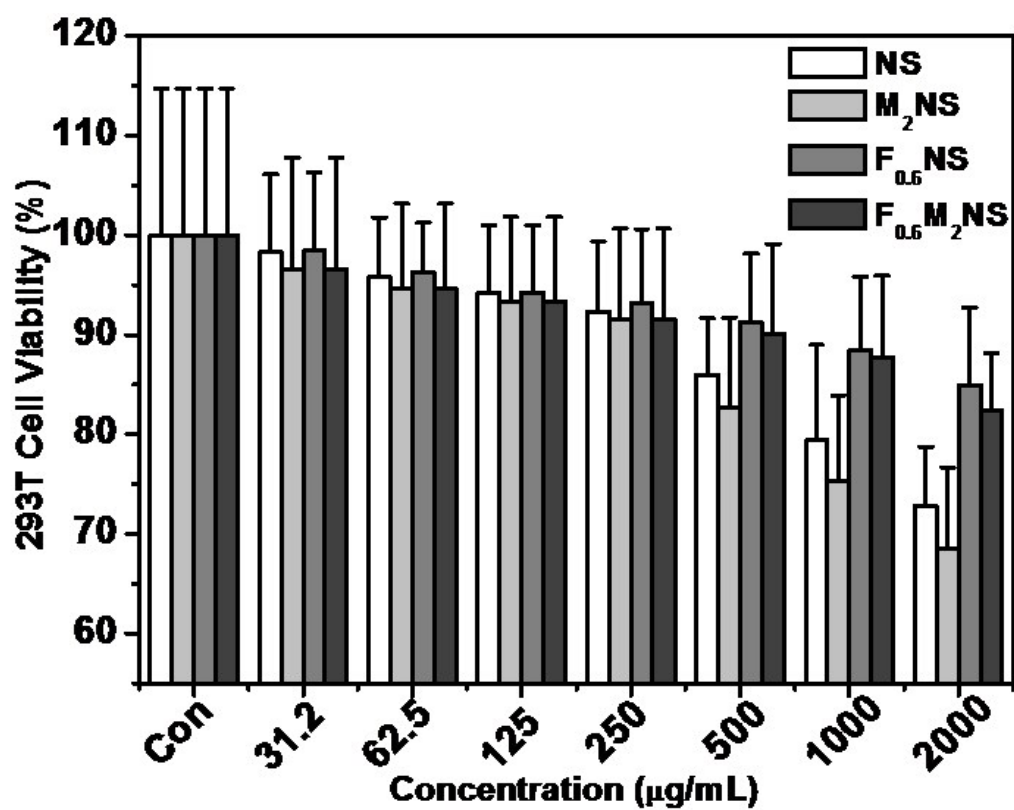
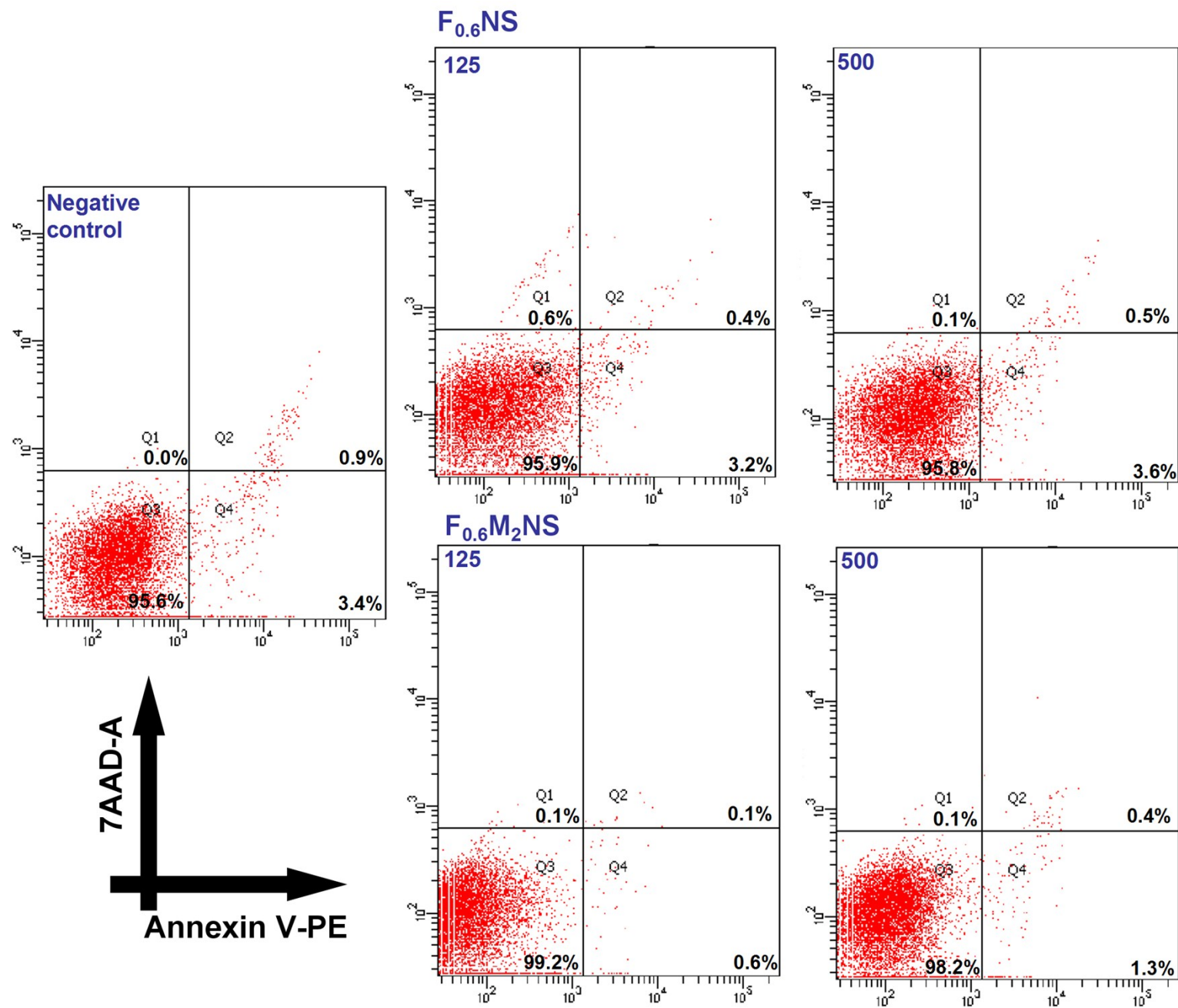
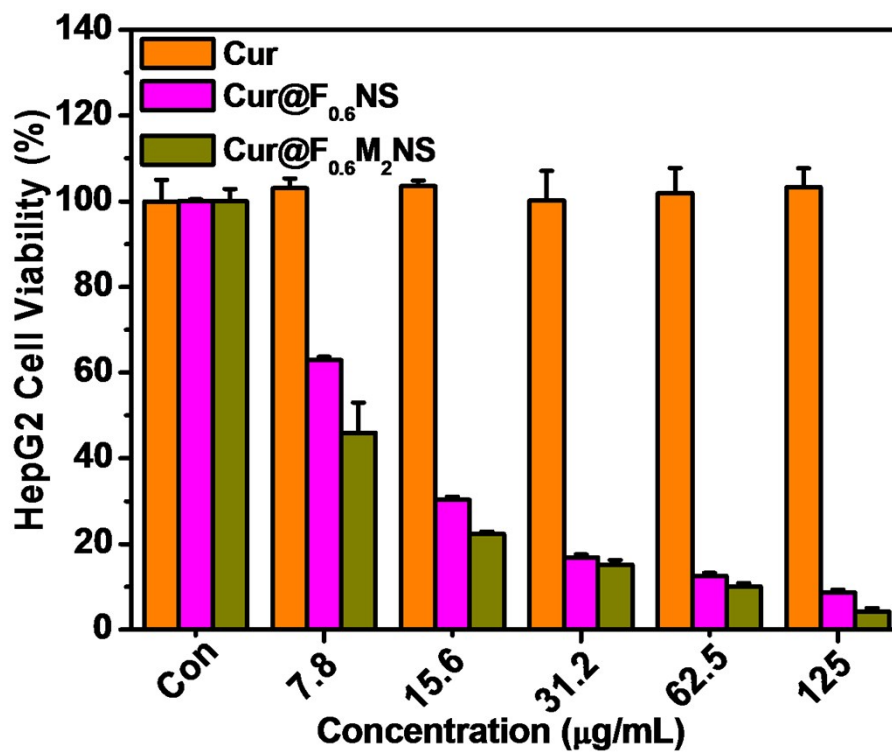


Fig .S11 *In vitro* 293T cell viability incubation with NS, M<sub>2</sub>NS, F<sub>0.6</sub>NS and F<sub>0.6</sub>M<sub>2</sub>NS for 48 h



**Fig .S12** The apoptosis induction by drug delivery materials, *i.e.*, F<sub>0.6</sub>NS and F<sub>0.6</sub>M<sub>2</sub>NS with different concentrations, such as 125 mg/L and 500 mg/L on SK-HEP1 cell line



**Fig .S13** *In vitro* HepG2 cell viability incubation with different drug formulations pure curcumin, Cur@F<sub>0.6</sub>NS and Cur@F<sub>0.6</sub>M<sub>2</sub>NS equal to curcumin concentrations (ranging from 7.8 to 125 µg/mL) for 48 h.

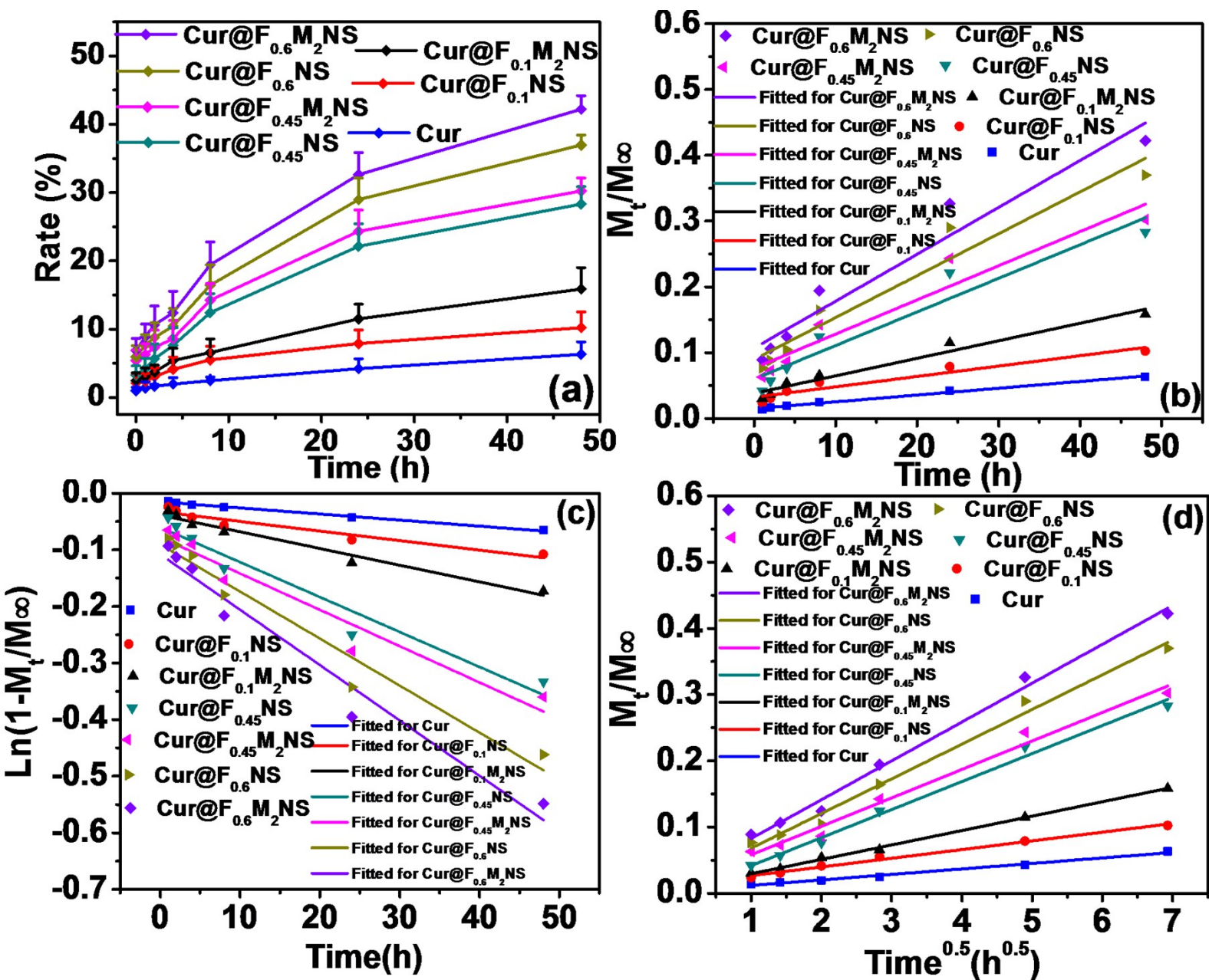


Fig . S14 Drug release of different curcumin formulations in 0.5 % SLS (a), Fitted of different models for different formulations of curcumin release in 0.5 % SLS with Zero-order model(b), First-order (c) and Higuchi model (d)

**Table. S3** Pharmacokinetics of different drug deliver nanosystems release *in vitro*

Models	Drug Formulation	Equation	R <sup>2</sup>
Zero-order ( $M_t/M_\infty = kt + K$ )	Cur	$M_t/M_\infty = 0.00103t + 0.01504$	0.9891
	Cur@F <sub>0.1</sub> M <sub>2</sub> NS	$M_t/M_\infty = 0.00266t + 0.03829$	0.9559
	Cur@F <sub>0.1</sub> NS	$M_t/M_\infty = 0.00158t + 0.03242$	0.9031
	Cur@F <sub>0.6</sub> M <sub>2</sub> NS	$M_t/M_\infty = 0.00713t + 0.10708$	0.9324
	Cur@F <sub>0.6</sub> NS	$M_t/M_\infty = 0.00637t + 0.08986$	0.9289
	Cur@F <sub>0.45</sub> M <sub>2</sub> NS	$M_t/M_\infty = 0.00519t + 0.07649$	0.9097
	Cur@F <sub>0.45</sub> NS	$M_t/M_\infty = 0.00511t + 0.05988$	0.9146
Higuchi ( $M_t/M_\infty = kt^{0.5} + b$ )	Cur	$M_t/M_\infty = 0.0083t^{0.5} + 0.00365$	0.9869
	Cur@F <sub>0.1</sub> M <sub>2</sub> NS	$M_t/M_\infty = 0.02176t^{0.5} + 0.00774$	0.9976
	Cur@F <sub>0.1</sub> NS	$M_t/M_\infty = 0.01313t^{0.5} + 0.01356$	0.9885
	Cur@F <sub>0.6</sub> M <sub>2</sub> NS	$M_t/M_\infty = 0.05868t^{0.5} + 0.02394$	0.9913
	Cur@F <sub>0.6</sub> NS	$M_t/M_\infty = 0.05240t^{0.5} + 0.01561$	0.9876
	Cur@F <sub>0.45</sub> M <sub>2</sub> NS	$M_t/M_\infty = 0.04299t^{0.5} + 0.01513$	0.9822
	Cur@F <sub>0.45</sub> NS	$M_t/M_\infty = 0.04234t^{0.5} - 0.00062$	0.9896
First-order ( $\ln(1-M_t/M_\infty) = -kt + b$ )	Cur	$\ln(1-M_t/M_\infty) = -0.00108t - 0.01505$	0.9906
	Cur@F <sub>0.1</sub> M <sub>2</sub> NS	$\ln(1-M_t/M_\infty) = -0.00295t - 0.03846$	0.9638
	Cur@F <sub>0.1</sub> NS	$\ln(1-M_t/M_\infty) = -0.00169t - 0.03282$	0.9106
	Cur@F <sub>0.6</sub> M <sub>2</sub> NS	$\ln(1-M_t/M_\infty) = -0.00978t - 0.10785$	0.9592
	Cur@F <sub>0.6</sub> NS	$\ln(1-M_t/M_\infty) = -0.00832t - 0.09033$	0.9511
	Cur@F <sub>0.45</sub> M <sub>2</sub> NS	$\ln(1-M_t/M_\infty) = -0.00642t - 0.07755$	0.9290
	Cur@F <sub>0.45</sub> NS	$\ln(1-M_t/M_\infty) = -0.00618t - 0.05983$	0.9342

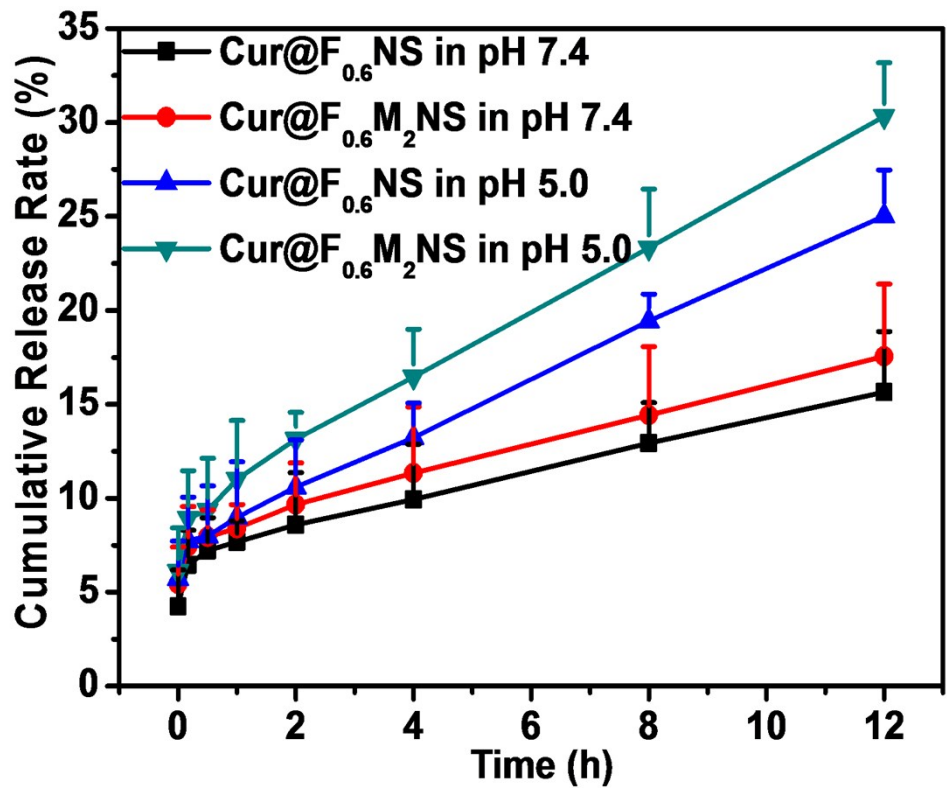
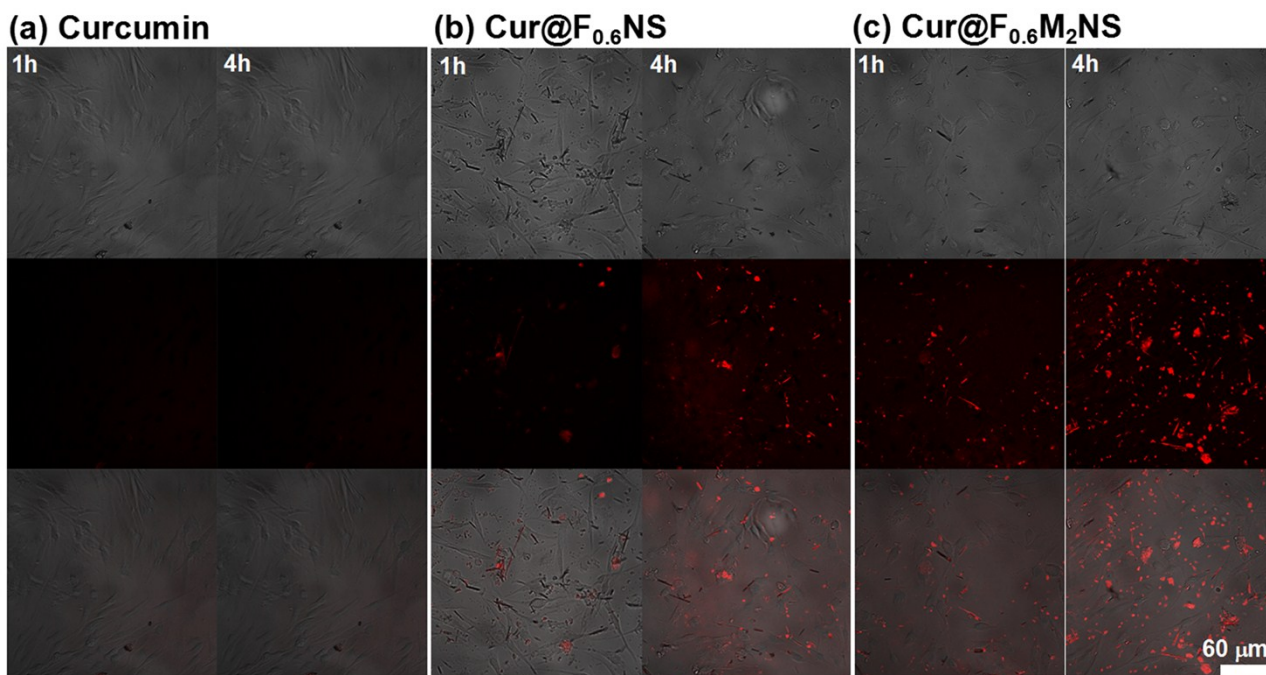


Fig . S15 Drug release of different curcumin formulations in different PBS medium



**Fig .S16** Fluorescence confocal images of free curcumin, Cur@F<sub>0.6</sub>NS and Cur@F<sub>0.6</sub>M<sub>2</sub>NS uptake by SK-HEP1 cells in 1 and 4 h. From top to bottom: bright-field image, fluorescence image and merged image. Scale bar: 60 μm.

F. Liu, J. N. Wang, Q. Y. Cao, H. D. Deng, G. Shao, D. Y. B. Deng and W. Y. Zhou, *Chem. Comm.*, 2015, **51**, 2357-2360.

F. Liu, J. N. Wang, P. L. Huang, Q. Zhang, J. T. Deng, Q. Y. Cao, J. T. Jia, J. H. Cheng, Y. P. Fang, D. Y. B. Deng and W. Y. Zhou, *J. Mater. Chem. B*, 2015, **3**, 2206-2214.

P. L. Huang, J. N. Wang, S. T. Lai, F. Liu, N. Ni, Q. Y. Cao, W. Liu, Deng, D. Y. B. Deng and W. Y. Zhou, *J. Mater. Chem. B*, 2014, **2**, 8616-8625.

A. F. Wang, F. Muhammad, W. X. Qi, N. Wang, L. Chen and G. S. Zhu, *ACS Appl. Mater. Interfaces.*, 2014, **6**, 14377-14383